

Cyclic variations in the main components of the solar large-scale magnetic field

V. N. Obridko,^{1★} D. D. Sokoloff,^{1,2★} B. D. Shelting,¹ A. S. Shibalova^{1,2}
and I. M. Livshits^{1,3}

¹*IZMIRAN, Kaluzhskoe shosse, 4, Troitsk, Moscow 142191, Russia*

²*Department of Physics, Lomonosov Moscow State University, Moscow 119991, Russia*

³*Sternberg State Astronomical Institute, Lomonosov Moscow State University, Moscow 119991, Russia*

Accepted 2020 January 14. Received 2020 January 14; in original form 2019 October 21

ABSTRACT

We consider variations of the dipole and quadrupole components of the solar large-scale magnetic field. Both axial and equatorial dipoles exhibit a systematic decrease during the past four cycles, in accordance with the general decrease of solar activity. The transition of the pole of a dipole from the polar region to the midlatitudes occurs rather quickly, so that the longitude of the pole changes little. With time, however, this inclined dipole region shifts to larger longitudes, which suggests an acceleration of dipole rotation. The mean rotation rate exceeds the Carrington velocity by 0.6 per cent. The behaviour of a quadrupole differs dramatically. Its decrease over the last four cycles was much smaller than that of the dipole moment. The ratio of the quadrupole and dipole moments has increased for four cycles more than twice, in contrast to sunspot numbers, which displayed a twofold decrease for the same time interval. Regarding quadrupole rotation, the mean longitude of the poles of one sign decreased by 600° over four cycles, which suggests that the mean rotation rate was lower than the Carrington velocity by 0.28 per cent. We do not, however, see any conclusive evidence that, in the period under discussion, a mode of quadrupole symmetry was excited in the Sun along with the dipole mode.

Key words: dynamo – Sun: activity – Sun: magnetic fields.

1 INTRODUCTION

It is generally agreed that most of the principal active phenomena in the Sun are due to the evolution of local magnetic fields. This evolution results in the formation of sunspots and active regions, i.e. features of a few arcsec in size. Solar features of a larger scale are not seen in high-resolution images; however, they are clearly revealed on Stanford synoptic charts, which have resolution 3×3 arcmin². On magnetic charts, one can conventionally isolate local (a few arcmin) and large-scale (from several to 10×10 arcmin² to 20×20 arcmin², i.e. $\approx 0.2R_\odot$) magnetic fields. A large-scale field involves two high-latitude regions occupied by fields of opposite sign and a set of quasi-unipolar structures at mid and low latitudes. Quasi-unipolar magnetic regions, which are sometimes the remnants of large active regions, live from half a year to 1–2 years. The largest scale is associated with the dipole component of the magnetic field – the global dipole.

It has long been known, above all, from eclipse observations that, at very low activity, the magnetic field in the corona is, under

certain approximations, a global dipole, the axis of which almost coincides with the rotation axis of the Sun. Here, we mean the coronal layers where the solar wind speed is still small, i.e. the layers below the solar wind ‘source surface’. In this phase of the cycle, the disturbing effect of local fields on the dipole is weak. Such a magnetic configuration remains stable for a few years. Due to the dipole configuration of the global field, a number of high coronal loops connecting fields of opposite polarity on both sides of the equator arise in the low-latitude zone. This forms the well-known large-scale structure of the solar corona at its minimum, which includes a belt of streamers at all longitudes in the vicinity of the equator and two systems of polar plumes. The global magnetic fields carried out to interplanetary space by the solar wind form the heliospheric current sheet, which separates oppositely directed magnetic fluxes. In periods of low activity, this neutral current sheet is flat. With the rise of activity, the influence of active regions increases and the polarity separation line between large-scale fields in the vicinity of the equator becomes wavy. In addition, the role of quadrupole and higher-order harmonics of large-scale magnetic fields also increases during this period.

It is convenient to estimate the contribution of magnetic fields of different scales by studying cyclic variations in the characteristics of

* E-mail: obridko@izmiran.ru (VNO); sokoloff.dd@gmail.com (DDS)

different multipoles. In particular, it is important that their rotation be analysed separately. The dependence of dynamo characteristics on rotation was considered in Noyes et al. (1984), Saar & Brandenburg (1999), Pizzolato et al. (2003), Böhm-Vitense (2007) and Reiners, Basri & Browning (2009). Some authors have shown that there is also an inverse effect – a negative correlation between the magnetic field and rotation velocity (Hathaway & Wilson 1980; Kambry & Nishikawa 1990; Howard 1984; Gigolashvili & Khutsishvili 1990; Obridko & Shelting 2016).

The relationship between fields of different scales and the characteristics of solar activity was studied by considering mainly low-order multipoles – the dipole and quadrupole. Stenflo & Vogel (1986), Stenflo & Weisenhorn (1987), Stenflo & Güdel (1988) and Knaack & Stenflo (2005) arrived at the conclusion that large-scale fields are based on spherical antisymmetric harmonics, such as the axial dipole and octupole.

Livshits & Obridko (2006) used data on large-scale magnetic fields (synoptic charts) and the field of the Sun as a star (general magnetic field) to determine the magnetic moment and direction of the dipole field for the past three solar cycles (21–23). It was found that both the magnitude of the moment and its vertical and horizontal components changed regularly during a cycle, never turning to zero. The process of polarity reversal of the global dipole is a change in the inclination of its axis, which is not smooth, but occurs in a few stages lasting 1–2 years. Before the reversal begins, the dipole axis executes a precession about the solar rotation axis and then moves in the meridional plane to reach very low latitudes, where it begins to shift significantly in longitude. The vector of the global dipole precesses (not too regularly) about the direction of the rotation axis. Then, during polarity reversal, it turns round virtually in the meridian plane, i.e. at the same heliolongitude in each hemisphere. The amplitudes of the two components change differently. The vertical component changes smoothly, reaching its maximum absolute value at the minimum of the cycle (vertical dipole). The horizontal component determines the maximum value of the total dipole field in epochs of high activity. It is more variable and actually determines the direction of the full vector of the dipole field in the process of polarity reversal.

The characteristics of both the full vector of the dipole moment and its components change depending on the phase of the cycle.

In addition to the main oscillation mode – quasi-11-year cycle – apparently, shorter oscillation periods exist. Fluctuations of the magnetic moment of horizontal and vertical dipoles during a quasi-11-year cycle are exactly the same. Livshits & Obridko (2006) believe that complete coincidence in both period and amplitude indicates essentially the same physical phenomenon, and separation into two types does not have much physical sense from the point of view of the main cycle of solar activity. We are therefore dealing here with cyclic changes in the latitude of the inclined rotator. The situation is completely different when fluctuations with periods of 1.3–2.5 years are concerned. These modes are present only in oscillations of the magnetic moment of the horizontal dipole and are absent in oscillations of the vertical dipole. Their existence is responsible for variations in the tilt of the total dipole.

Similar results were reported by De Rosa, Brun & Hoeksema (2012). These authors used the same observation data from the John Wilcox Solar Observatory (WSO) as Livshits & Obridko (2006) and coefficients obtained using the Potential-Field Source-Surface Model (PFSS). The data covered three activity cycles (21, 22 and 23) and the problem was considered more broadly, including higher-order harmonics.

The evolution of the first harmonics of the solar magnetic field is not only interesting in itself, but also of particular value as a basis for comparing theoretical ideas in the study of the solar dynamo with observational data. The fact is that the solar dynamo is operating somewhere under the solar surface. It is generally believed that this occurs in the inversion layer (e.g. Choudhuri 1990); however, it may also be a layer not very far from the surface (e.g. Brandenburg 2005). It is possible that there are two zones of generation. However, the magnetic fields that are seen on the surface in the form of sunspots and the large-scale magnetic field differ significantly in their configuration from those that are generated directly by the solar dynamo. For example, an isolated sunspot is a local feature and does not belong to the surface large-scale magnetic field, while all sunspots together for a period comparable with an 11-year cycle form (as seen on butterfly diagrams) a large-scale structure, which gives us an idea of the evolution of the toroidal magnetic field. Therefore, a comparison with solar dynamo models requires that we consider the evolution of the mean parameters of the solar surface magnetic field.

The basic concepts of solar dynamo theory were formulated in terms of the mean magnetic field (e.g. Krause & Rädler 1980). At present, of course, a detailed numerical simulation of the solar dynamo is possible (e.g. Brandenburg, Sokoloff & Subramanian 2012); however, when interpreting the results of such a simulation, we have to turn to the behaviour of the mean large-scale field parameters. In this context, it is necessary to distinguish between mean and instantaneous values of the solar magnetic dipole moment during its inversion (Moss, Kitchatinov & Sokoloff 2013; Pipin et al. 2014), which emphasizes the complexity of the problem under consideration.

Of particular interest to dynamo theory is the behaviour of the two first harmonics (odd and even) of the solar magnetic field, i.e. the dipole and quadrupole. The fact is, there are two types of magnetic field (odd and even with respect to the solar equator) that can be excited in a convection shell strictly symmetric about the equator. In the process, neither meridional circulation nor differential rotation and mirror asymmetry of motions mix these fields. Of course, the odd and even configurations cannot be reduced to a pure dipole or quadrupole, if only because they include a toroidal magnetic field. However, the behaviour of the magnetic dipole and quadrupole can illustrate the evolution of these configurations in time.

In particular, in the simplest models of the solar dynamo, both the quadrupole moment and the higher-order even modes are exactly zero. A minor change in the hydrodynamics of the spherical shell will allow us to simulate the generation of magnetic fields of dipolar rather than quadrupolar symmetry (see Moss, Saar & Sokoloff 2008, and references therein). It would be natural to suggest that there may be stars in which this type of dynamo mechanism operates. Possibly, recent Zeeman–Doppler observations of complex structures of stellar magnetic fields (Rosén et al. 2016, 2018) support this expectation, however this point deserves to be addressed in a special article. In principle, the dynamo mechanism can also produce mixed parity solutions (e.g. Jennings & Weiss 1991). This, probably, is how the solar dynamo worked at the end of the Maunder minimum (see Sokoloff & Nesme-Ribes 1994; Usoskin et al. 2015, and references therein).

The magnetic field of the Sun, obviously, contains modes of both dipolar and quadrupolar symmetry. In principle, we could suggest that the solar dynamo constantly produces a mixed parity configuration, but at the end of the Maunder minimum the contribution of quadrupolar modes was abnormally large. However, another point of view is possible, according to which quadrupolar modes arise

simply because the Sun is not perfectly symmetric with respect to the solar equator. Checking which hypothesis is better supported by observations will, obviously, require a study of the time evolution of the solar quadrupolar moment.

In this article, which is, in some sense, a development of the ideas of Livshits & Obridko (2006), we will focus on the analysis of the joint evolution of the basic odd (dipole) and basic even (quadrupole) harmonics. It is important to note that we now have at our disposal data for four activity cycles.

2 FORMULATION OF THE PROBLEM AND BASIC EQUATIONS

Using WSO synoptic charts of the radial component of the solar magnetic field (Scherrer & Wilcox 1977), we calculated the magnetic field in the potential approximation by the well-known method described in Hoeksema & Scherrer (1986) and Hoeksema (1991) in its classical version, without assuming a radial field in the photosphere. WSO measurements of the magnetic-field longitudinal component¹ were used as the source data to plot the synoptic charts for each Carrington rotation. The WSO data used in this study cover a time interval of 43 years from the beginning of Carrington rotation (CR) 1642 (1976 May 27) to the end of CR 2210 (2018 November 23).

The coronal magnetic field was extrapolated by solving the boundary problem with the line-of-sight field component measured in the photosphere and a strictly radial field at the source surface. For the source surface we have taken a conventional boundary, where the potential approximation ceases to be true and the field lines are carried away radially by the solar wind. At this boundary, the magnetic field is assumed to be normal to the surface and the potential is zero. Of course, the position of this conventional boundary can be fixed only approximately and is usually assumed to be located at a distance of 2.5 radii from the centre of the Sun. This allowed us to calculate three magnetic-field components in spherical coordinates B_r , B_θ , B_φ . The magnetic-field components have the following form:

$$B_r = \sum P_n^m(\cos\theta)(g_{nm} \cos m\varphi + h_{nm} \sin m\varphi) \times [(n+1)(R_\odot/R)^{n+2} - n(R/R_s)^{n-1}c_n], \quad (1)$$

$$B_\theta = - \sum \frac{\partial P_n^m(\cos\theta)}{\partial\theta}(g_{nm} \cos m\varphi + h_{nm} \sin m\varphi) \times [(R_\odot/R)^{n+2} + (R/R_s)^{n-1}c_n], \quad (2)$$

$$B_\varphi = - \sum \frac{m}{\sin\theta} P_n^m(\cos\theta)(h_{nm} \cos m\varphi - g_{nm} \sin m\varphi) \times [(R_\odot/R)^{n+2} + (R/R_s)^{n-1}c_n]. \quad (3)$$

Here, $0 \leq m \leq n \leq N$ (usually, $N = 9$); $c_n = -(R_\odot/R_s)^{n+2}$, where R_\odot and R_s are the solar radius and the radius of the source surface, respectively, measured from the centre of the Sun; P_n^m are the Legendre polynomials; g_{nm} and h_{nm} are the coefficients of the spherical harmonic analysis obtained by comparison with observations at the photospheric level. It is usually assumed that $R_\odot = 1$ and $R_s = 2.5$. It is important to note that the coefficients were calculated under the assumption that the field is potential throughout the photosphere up to the source surface, including the boundaries. At the source surface, the field is assumed to be strictly radial. The source surface is taken at a distance of 2.5 solar radii

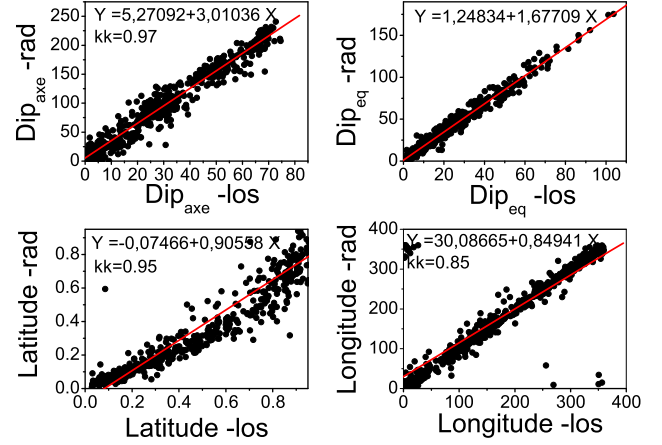


Figure 1. Comparison of the dipole parameters calculated in the classical and radial systems.

from the centre of the Sun. The results obtained according to this scheme on the site <http://wso.stanford.edu/synopticl.html> are called ‘classical’.

In fact, our calculations yield the corresponding harmonics rather than the classical multipoles. As is known, direct WSO measurements provide the longitudinal component of the magnetic field. In order to obtain the expansion coefficients, we find the expression for the longitudinal component from equations (1) – (3). In this expression, the coefficients have not yet been determined. Then the expansion coefficients are found by assuming $R = R_\odot$ and taking into account the orthogonality of the polynomials, or directly by applying the least-squares method. The coefficients obtained, naturally, differ from the coefficients of the contribution of classical multipoles. One cannot expect that such a distorted multipole would rotate as a single piece, since the terms determining the dependence on the source surface radius are involved in calculations of the coefficients. They are different in equation (1) and equations (2) – (3). The ratio of the components varies with height; therefore, the rotation of the ‘dipole’ cannot be identified with the rotation of the pole. However, these differences are small enough to ignore and we will continue using the expressions ‘dipole’ and ‘quadrupole’ instead of the more precise terms ‘first harmonic’ and ‘second harmonic’.

Some authors (see the discussion in Wang & Sheeley 1992) have pointed out the shortcomings of the classical method and proposed the hypothesis of a radial magnetic field in the photosphere. The ‘radial’ computation assumes that the field in the photosphere is radial. Our estimates (Obridko, Shelting & Kharshiladze 2006) have shown that, when these two methods are used, differences exist and mainly concern the magnetic field intensity. As a rule, the first harmonics are much larger than in the classical method. On the other hand, the differences in the structure of the field lines are insignificant, especially over long time intervals. It can therefore be assumed that the rotation characteristics we find do not depend strongly on the method applied. A slight difference between the results obtained by these two methods is noticeable at latitudes higher than 70° .

Fig. 1 compares the magnetic moments of (a) axial and (b) equatorial dipoles, (c) the cosine of latitude and (d) the longitude of the north pole for both systems. The abscissa shows the values in the classical system (the photospheric surface field is potential; the directly observed longitudinal field is used). The ordinates indicate similar values obtained under the assumption that the field in the

¹<http://wso.stanford.edu/synopticl.html>

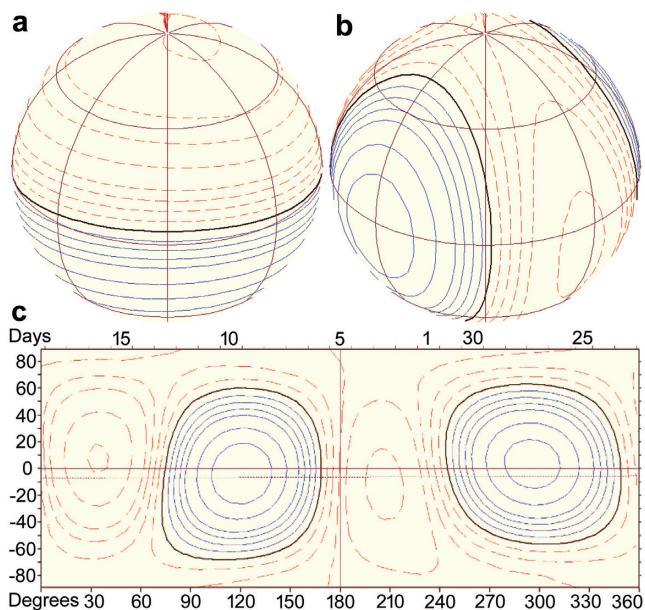


Figure 2. Contour maps of (a) a dipole and (b,c) a quadrupole.

photosphere is radial. The calculations were performed for rotations from 1642–2210 without averaging. In all cases, one can see a very high correlation. However, the moment of the axial dipole is three times greater in the case of the radial hypothesis. The equatorial dipole in the radial hypothesis is greater by a factor of 1.67. The longitudes and latitudes agree. A deviation from linear dependence for the latitude is due to the fact that the radial hypothesis underestimates the equatorial dipole.

A new software tool has been developed, which allows calculation of the structure of each harmonic separately. Generally speaking, the map of a quadrupole sometimes looks rather intricate. The simplest map is illustrated in Fig. 2. Two versions of representation are possible: we can plot either a 3D projection or a 2D map in Carrington coordinates. Fig. 2 shows maps of (a) the dipole and (b,c) the quadrupole for 2006 February 5. On the 3D maps, the axis is inclined in the way an observer might see it from a point located 30° above the plane of the equator. On the 2D map, the dotted line shows the cross-section of the disc by the ecliptic plane. Positive polarity (N) is coloured blue (gray) and negative polarity (S) red (dashed). The contour lines correspond to values of 0, 5, 10, 15, 20, 30, 40, 50, 70 and 100 microtesla (μT).

3 CYCLIC VARIATIONS OF A DIPOLE

In recent years, the dynamo theory and helioseismic studies have made significant progress. Unfortunately, these studies do not take into account fully the results of observation of magnetic fields in the Sun. In particular, when analysing the generation of the magnetic field in the solar interior, it was sometimes assumed that the dipole moment of the Sun disappears completely at the beginning of the field reversal near the solar maximum and then reappears with the opposite sign (Livshits & Obridko 2006). This urged us to return to analysis of the contribution of the dipole component to the observed magnetic field of the Sun (see also Pipin et al. 2014).

The axial dipole is largest at the minimum of the cycle at high latitudes. The equatorial dipole reaches its maximum at the maximum of the cycle, mainly at low latitudes. The cyclic variation in the value of the unsigned magnetic field of the axial, $B_d(ax)$, and

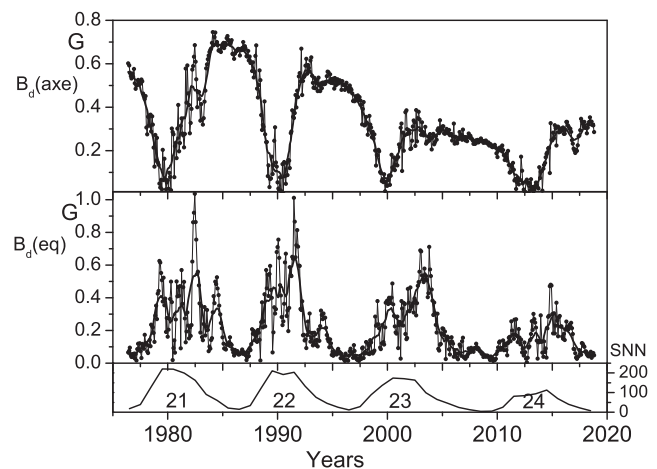


Figure 3. Cyclic variation of the axial, $B_d(ax)$, and equatorial, $B_d(eq)$, dipoles. The lower panel shows the sunspot numbers, SSN (Version 2).

equatorial, $B_d(eq)$, dipoles averaged over the entire solar surface is shown in Fig. 3.

As seen from Fig. 3, this simplified description needs clarification. The three main characteristic points of the cycle do not coincide. The sunspot maximum of Cycle 21 was recorded in 1979 December. The double maximum of the equatorial dipole (1979 May and 1982 August) does not coincide with this date. Between both dates, there is a deep gap of the Gnevyshev gap type (1979 April). The date of reversal of the axial dipole is close to this gap (1979 December) and to the date of the sunspot maximum, but is far ahead of the date of the main maximum of the equatorial dipole. In Cycle 22, the maximum sunspot numbers (SSN) were recorded in 1989 July, which does not coincide with the reversal date (1990 April) nor with the main (secondary) maximum (1991 July). In Cycle 23, the SSN maximum took place in 2000 April. The reversal almost coincided with this date, but the maximum of the equatorial dipole was recorded much later (in 2003 April). In Cycle 24, the secondary SSN maximum was recorded in 2014 April, the reversal occurred in 2013 March and the maximum of the axial dipole took place in 2016 January. It should also be noted that the reversal of the polar field lasts rather a long time, while the sign reversal and, correspondingly, the minimum in Fig. 3(a) take a relatively short time.

The upper panel of Fig. 4 illustrates variations in the total magnetic moment of the dipole. The data were smoothed over 14 rotations.

The dipole magnetic moment M_{dip} , the axial dipole moment M_{ax} and the equatorial dipole moment M_{eq} are determined by the following equations:

$$M_{\text{dip}} = \sqrt{g_{10}^2 + g_{11}^2 + h_{11}^2}, \quad (4)$$

$$M_{\text{ax}} = |g_{10}|, \quad (5)$$

$$M_{\text{eq}} = \sqrt{g_{11}^2 + h_{11}^2}. \quad (6)$$

The middle panel of Fig. 4 shows the ratio of the smoothed values of equatorial and axial dipole moments. One can see that, in the vicinity of the cycle maximum, the moment of the equatorial dipole exceeds the moment of the axial dipole by an order of magnitude, while near the minimum the ratio is opposite. Since the dates of the extreme values of the dipole moments do not coincide, the total dipole not only never drops to zero, but is significant in magnitude

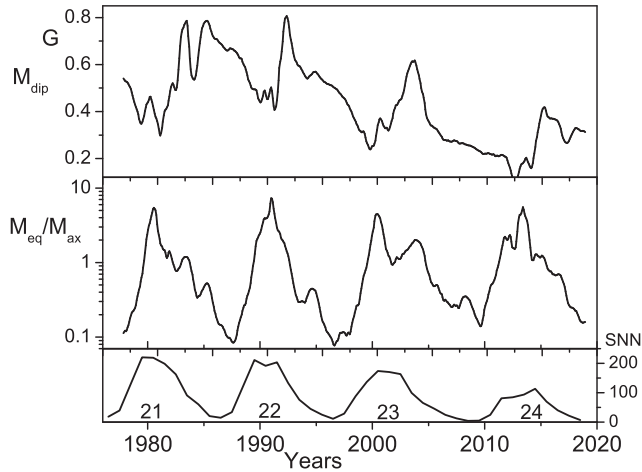


Figure 4. The dipole magnetic moment (upper panel) and the ratio of the equatorial and axial dipole moments (middle panel). The ordinate scale on the middle panel is logarithmic. The lower panel shows sunspot numbers (Version 2).

even near the minimum of the cycle. This led Livshits & Obridko (2006) to the conclusion that the dipole turns over and, thus, to the idea of an inclined rotator. This conclusion is true in principle, but not entirely accurate. The equatorial dipole cannot be considered a direct transform of the axial dipole. They differ significantly, not only in spatial orientation but also in many other properties. In particular, it should be noted that the widely known gradual decrease in solar activity in both sunspot numbers (see Figs 3 and 4, upper panels) and magnetic field intensity² is due to a strong decrease in the equatorial rather than axial dipole (in Cycle 24, the latter even somewhat increased). This may imply that the axial and equatorial dipoles reflect different aspects of magnetic field generation in the Sun.

4 THE POSITION OF THE NORTH POLE OF THE DIPOLE AND ITS VARIATIONS DURING A CYCLE

Let us now trace cycle variations in the position of the north pole of the solar total dipole in both latitude and longitude. By definition, the latitude of the pole of the axial dipole is $\pm 90^\circ$ and the longitude is not determined. For the vector of an equatorial dipole parallel to the equatorial plane, the latitude of the pole is always zero and the longitude is a significant characteristic. The position of the north pole of the total dipole on the sphere depends on the longitude of the horizontal dipole and the ratio of the absolute values of the vertical and horizontal components.

Fig. 5 represents the position of the north magnetic pole on the surface of the Sun for each Carrington rotation in Cycles 21–24 in polar coordinates (φ, θ) , where θ and φ are, respectively, the latitude and longitude of the point on the solar surface. Note that the polar regions in the figure look more stretched than the equatorial ones. The centre of the coordinate system is the heliographic pole of the corresponding hemisphere. Red (light) shows the position of the pole in the northern hemisphere and blue (dark) that in the southern hemisphere.

²<http://wso.stanford.edu/Polar.html>

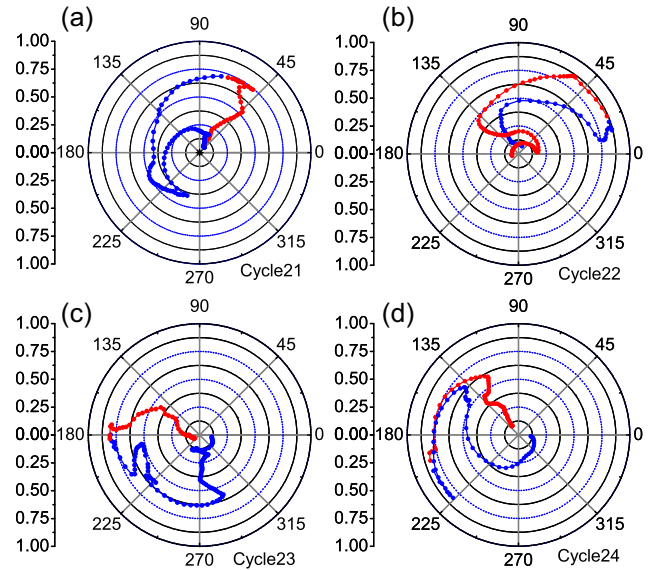


Figure 5. Positions of the north pole of the magnetic dipole in four solar activity cycles. The red (light) colour corresponds to the northern hemisphere, blue (dark) to the southern hemisphere. The diagrams show the northern (top) and southern (bottom) hemispheres of the Sun. The circles are contour lines of the values of $\cos\theta$ given on the vertical scales. The values of φ are given in degrees.

Similar diagrams for Cycles 21–23 in Livshits & Obridko (2006) show that, during the epoch of the minimum, the pole of the dipole executes fairly regular precession-like motions, making one or two turns relative to the rotation pole. This quasi-precession lasts for 1–3 years, during which the situation of the inclined rotator is realized. After that, a sharp jump (during 0.7–1.2 years) occurs into the equatorial region, where the dipole continues a smooth motion along the longitude for 1.5–3 years. Then a new jump occurs and precession continues at the opposite pole. The movement of the pole in the equatorial zone is rather complicated. De Rosa et al. (2012) called it ‘aimless wandering’, because it is determined by the random interaction of the active regions and the equatorial dipole. Livshits & Obridko (2006) revealed quasi-biennial variations in these seemingly random wanderings. Therefore, we have applied averaging over 27 Carrington rotations (corresponding quite precisely to two years) to plot Fig. 5. With this averaging, the picture becomes much clearer; one can see the full cycles described by the poles. Moreover, transit from high to low and medium latitudes occurs much faster and covers rather a narrow longitude range.

One can see a general counterclockwise latitudinal rotation. This means that the longitude increases, probably due to weak acceleration of the dipole rotation relative to the Carrington coordinates.

5 CHARACTERISTICS OF THE QUADRUPOLE

Fig. 6(a) represents the mean semiannual unsigned values of the magnetic field of the solar dipole ($l = 1$) averaged over the entire solar surface (B_d). As noted above, the maximum of the mean dipole values does not coincide in time with either the maximum of the polar field, which is observed in the vicinity of the sunspot minimum, or the sunspot maximum. The point is that we calculated the mean magnetic field of the total dipole, which consists of both axial and equatorial dipoles. The vertical (or axial) dipole peaks near the minimum of the sunspot cycle. The horizontal (or equatorial)

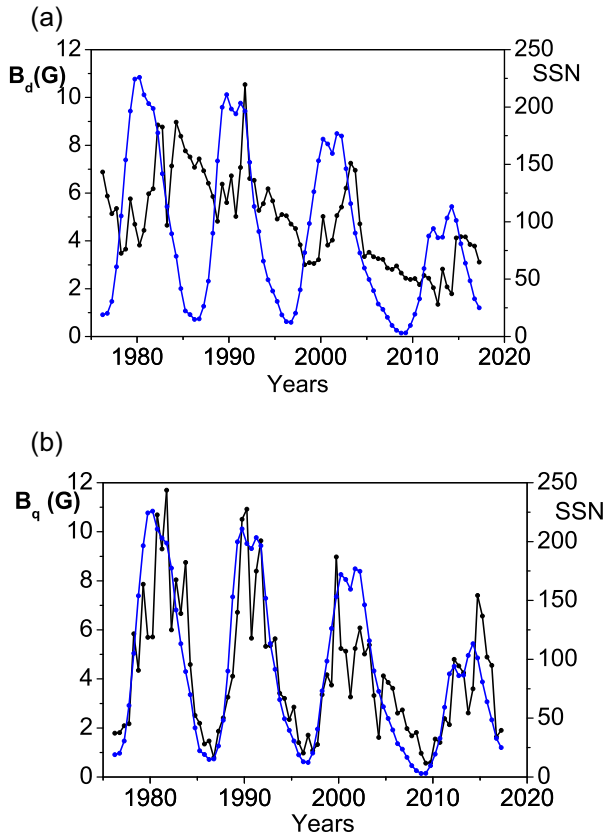


Figure 6. (a) Mean semiannual values of the magnetic field of the solar dipole ($l=1$; black curve) and (b) mean semiannual values of the magnetic pole of the solar quadrupole ($l=2$; black curve). The blue (gray) curves on both panels show the mean semiannual sunspot numbers (Version 2).

dipole reaches its maximum value near the maximum of the cycle. As a result, the maximum of the total dipole is observed at the beginning of the declining phase. Besides that, the magnetic field of the dipole is somewhat smaller than the maximum value of the polar field. This is due to the fact that the intensity of the polar field is determined not only by the axial dipole but also by other axisymmetric (odd relative to the equator) components.

At the sunspot maximum, the axial dipole tends to zero (polarity reversal occurs), while the equatorial dipole still exists at low latitudes. The ratio of the maximum to minimum dipole value is approximately 3:1.

Fig. 6(b) shows the mean semiannual unsigned values of the magnetic field of the solar quadrupole ($l=2$) averaged over the whole solar surface (B_q). The quadrupole reaches its maximum values in the vicinity of the sunspot maximum, sometimes slightly ahead (in Cycles 22 and 23) or behind it (in Cycles 21 and 24). A dramatic difference from the behaviour of the dipole is that, in epochs of minimum, the quadrupole field drops by an order of magnitude down to 0.1 G.

During the past four cycles of activity, the maximum values of the dipole and quadrupole have been decreasing. However the decrease in the quadrupole field was much smaller. As a result, the ratio B_q/B_d was increasing gradually (Fig. 7) and reached 3 in Cycle 24. This means that in Cycle 24 the quasi-symmetric dynamo generation mechanism proved to be more efficient. Note that such a relative increase in the contribution of the total component was recorded before the Maunder minimum (Ribes & Nesme-Ribes

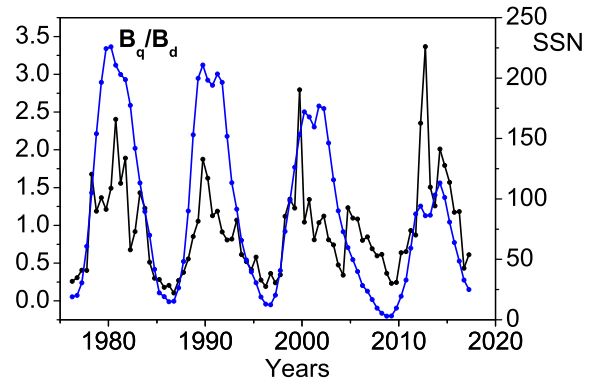


Figure 7. Ratio of the mean semiannual values of the magnetic field of the solar quadrupole B_q to the mean semiannual values of the magnetic pole of the solar dipole B_d . The blue (gray) curve shows sunspot numbers (Version 2).

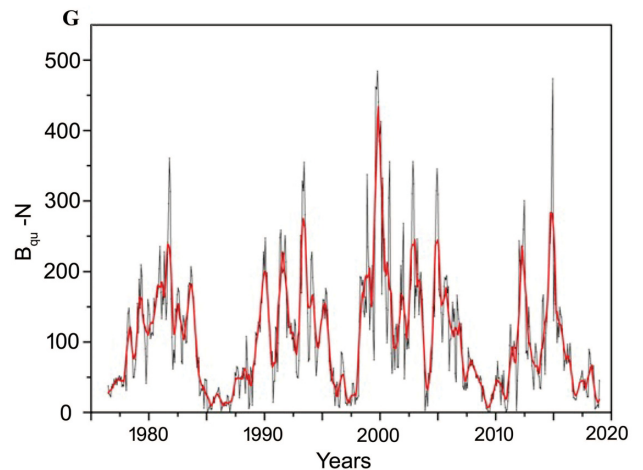


Figure 8. Magnetic field of the north pole of a quadrupole. The light-gray curve shows these values for one of the north poles. The red (dark-gray) curve shows the same values smoothed over seven rotations (i.e. about six months).

1993; Sokoloff & Nesme-Ribes 1994). It is instructive to note that, in other stars, Zeeman–Doppler imaging studies have revealed that the large-scale fields of stars tend to get more non-axisymmetric with increasing rotation rate (See et al. 2016) and persistent non-axisymmetric spot structures only appear on solar-type stars with high enough activity levels (Lehtinen et al. 2016).

Strictly speaking, the notion of the pole of a quadrupole requires a more precise definition. By analogy with the dipole, we mean by the pole of a quadrupole the point where the components B_ϕ and B_θ vanish and the field is strictly radial and reaches the maximum value. The quadrupole has four such points. In two of them, the field is positive; such points will be called poles N1 and N2. Similarly, the points with negative (‘southern’) field polarity are denoted as S1 and S2.

The values of the quadrupole magnetic field at the poles of one sign virtually coincide. The light-gray curve in Fig. 8 shows these values for one of the north poles. The red (dark-gray) curve shows the same values smoothed over seven rotations (i.e. about six months).

One can see a fine structure with the peaks shifted relative to each other by 2–3 years. We will return to this issue in Section 7.

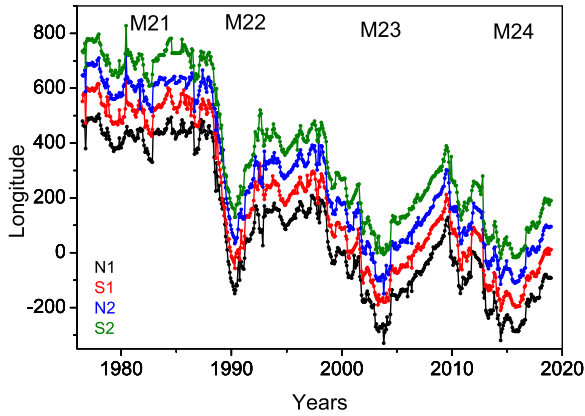


Figure 9. The longitude of four poles of a quadrupole.

Determining the longitude of a quadrupole rotating in the Carrington coordinate system is not an easy task. This is difficult to do analytically from equations (1)–(3). Therefore, we have used two methods.

(1) One is the method of joint minimization of B_ϕ and B_θ . For each rotation, we computed a grid of values of all three components of the quadrupole magnetic field and then found the coordinates of the four poles where these components were minimal. Unfortunately, this method may yield significant errors in the epochs of the activity minimum, when all components of the quadrupole magnetic field are close to zero. Besides this, certain difficulties arise when the longitude of a gradually moving quadrupole falls outside the range $0\text{--}360^\circ$ and a gap in the values occurs, which has to be filled in somehow.

(2) The second method is graphical. For each rotation, we plotted a map of all components of the magnetic field (one of the maps is represented in Fig. 2b) and found preliminary coordinates visually. Then the coordinates were specified by calculating the field values. This method is undoubtedly more laborious, but it provides additional data control and makes it easier to eliminate the uncertainty arising when the pole goes beyond $0\text{--}360^\circ$. Thus, we extend the notion of longitude, taking into account the prehistory of excursions of the pole.

The results obtained by both methods were brought together. The fact that, for physical reasons, the longitudes of the poles N_1 , S_1 , N_2 and S_2 must differ consecutively by 90° , 180° and 270° was used for additional control.

The values of the extended longitude obtained in such a way are shown in Fig. 9. The zero-point of the longitude scale corresponds to the beginning of rotation 2025 (2005 January 2). The total range of changes of each pole for four rotations was about 700° , i.e. approximately two Carrington rotations.

These calculations infer two important conclusions.

(1) One can notice a gradual decrease in longitude by about 600° in the same phases of the cycle over 42 years (i.e. over 567 rotations). This may mean a secular slowdown of the quadrupole by 1° per rotation (i.e. by 0.28 per cent). On large time-scales, this effect can be significant.

(2) The rotation rate of the quadrupole depends on the phase of the cycle. On the ascending branch of the activity cycle, the longitude decreases and therefore the rotation rate is lower than Carrington. After the maximum, it becomes higher than Carrington. At the minimum, the longitude does not change for some time

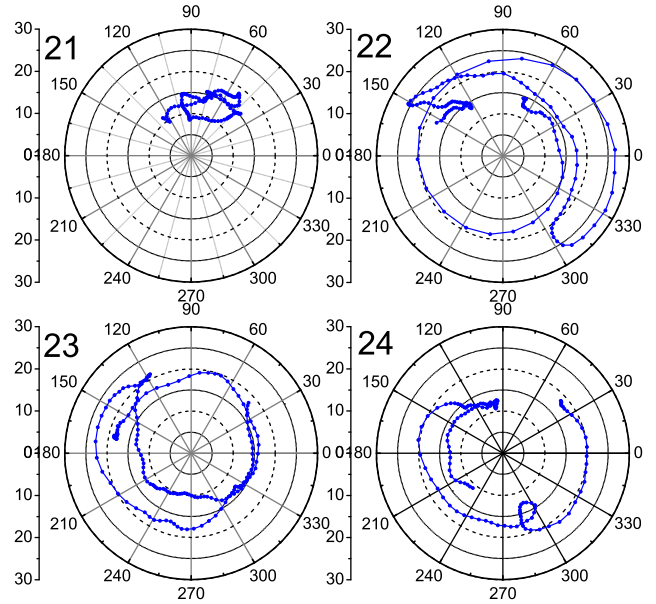


Figure 10. Relationship between the longitude and latitude of the pole of a quadrupole.

(occasionally quite a long period, as between Cycles 22 and 23) and the dipole takes a stable position in this coordinate system. This effect is visible in all cycles, but in Cycle 21 it is rather weak.

This may be due to the fact that the pole of a quadrupole moves in latitude. Fig. 10 shows the relationship between the longitude and latitude of the pole. To simplify the picture, we smoothed the data over 27 rotations, i.e. over a window of about two years. In doing so, we were taking into account the absolute value of the latitude, which is indicated in the figure in degrees. The generalized longitude is reduced to the range $0\text{--}360^\circ$. One can see that, at the beginning of the cycle, the pole moves clockwise (the rotation rate decreases); in the second part of the cycle, the direction of motion is reversed, i.e. the rotation rate increases. Moreover, the pole in the first part of the cycle is mostly located at high latitudes, where the rotation rate calculated following the differential rotation law is lower than the Carrington velocity, while in the second part the latitude drops. It is difficult to say whether the variations in the quadrupole rotation rate are limited to this effect, since the quadrupole itself is not a direct result of the existence of active regions.

The Carrington coordinates we are using in the Sun are referred to a latitude of 16° . For latitudes closer to the equator, the rotation period is smaller (i.e. higher rotation rate) and vice versa for higher latitudes. Fig. 11 represents the distribution of the longitudinally averaged surface magnetic field over the last four solar cycles (from <http://solarcyclescience.com/solarcycle.html>). We have added two solid black lines to the figure to show the Carrington latitudes. The shift of the centre of gravity of the activity to the equatorial zone results in a decrease in period and the corresponding longitude in Figs 9 and 12. However, this effect cannot explain differences in the rotation of the dipole and quadrupole fully.

6 ROTATION OF THE DIPOLE AND QUADRUPOLE

As mentioned above, a secular deceleration of the quadrupole rotation is observed over a long time interval. In the case of the dipole, this effect is absent or has the opposite sign.

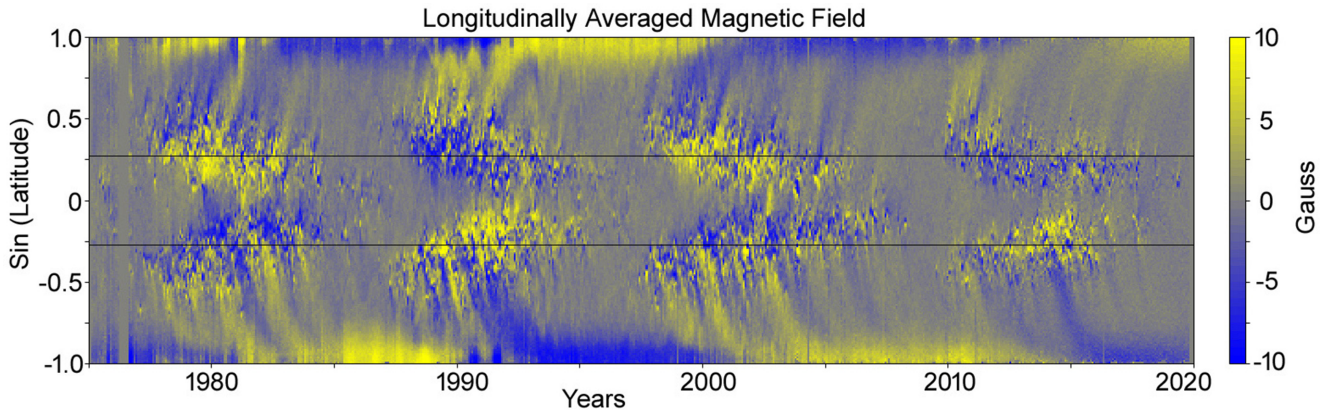


Figure 11. Distribution of the surface magnetic field (longitudinally averaged) over the last four solar cycles (from <http://solarcyclescience.com/solarcycle.html>).

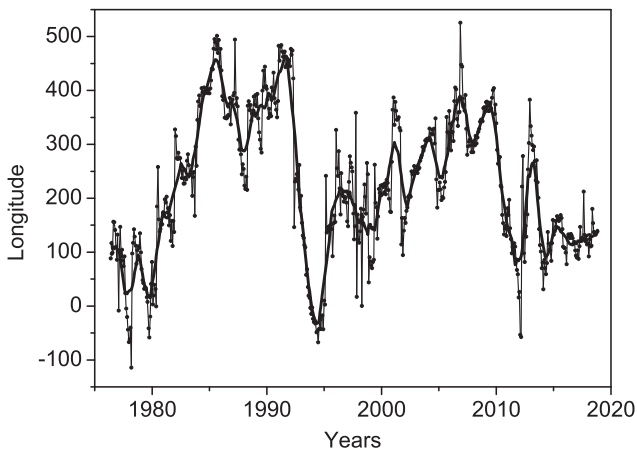


Figure 12. Longitude of the dipole north pole.

For 16 years from 1976–1992, the longitude of the dipole pole was gradually increasing, i.e. the rotation rate exceeded the Carrington velocity by about 0.6 per cent. After that, very fast reconstruction occurred, followed by a return to the previous position and, again, accelerated rotation at about the same velocity.

Against this background, both the dipole and the quadrupole display minor velocity fluctuations. The position of the longitude as a function of time is shown in Fig. 12.

The diagrams in Fig. 13 seem very much alike, but upon careful examination of this figure, together with Figs 9 and 12, it becomes clear that the dipole rotates predominantly counterclockwise, while the quadrupole changes its direction of rotation many times. This reflects the rotation of these two multipoles in the Carrington system. That is, in addition to the main rotation modes, there is also a finer structure. Variations in the rotation rate can be studied directly from the data represented in Figs 9 and 12.

Let us introduce the parameter

$$R(i) = [\varphi(i + 1) - \varphi(i - 1)]/720, \quad (7)$$

where i is the number of the following Carrington rotation and $\varphi(i)$ is the longitude. The parameter R introduced in this equation means the percentage deviation from the Carrington rotation rate over a small time interval. A positive value corresponds to a higher rotation rate and a negative one to a lower rotation rate.

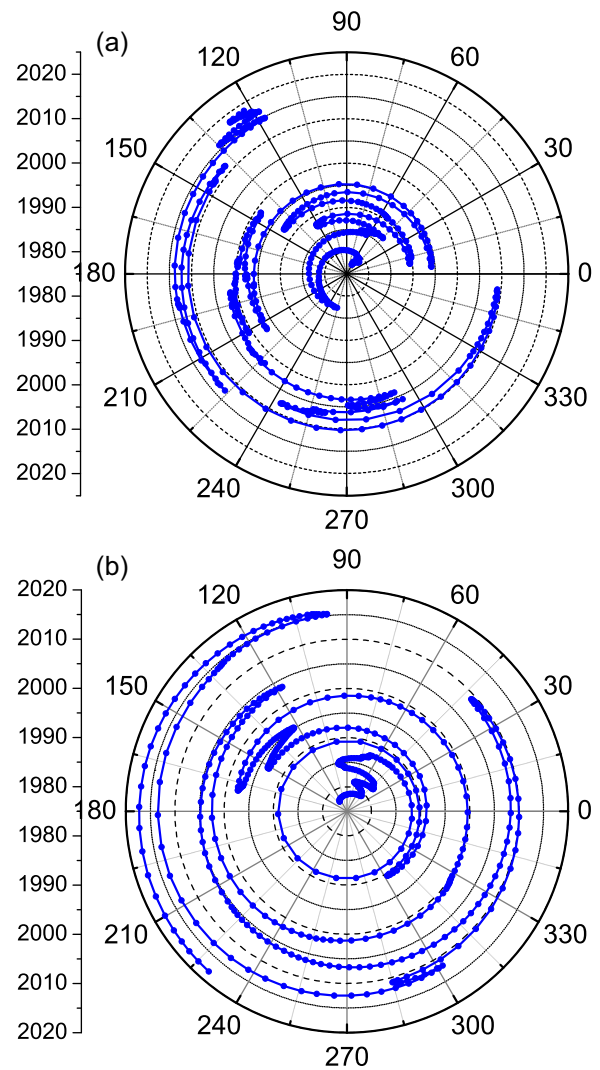


Figure 13. Longitude–time diagram for (a) the dipole and (b) the quadrupole.

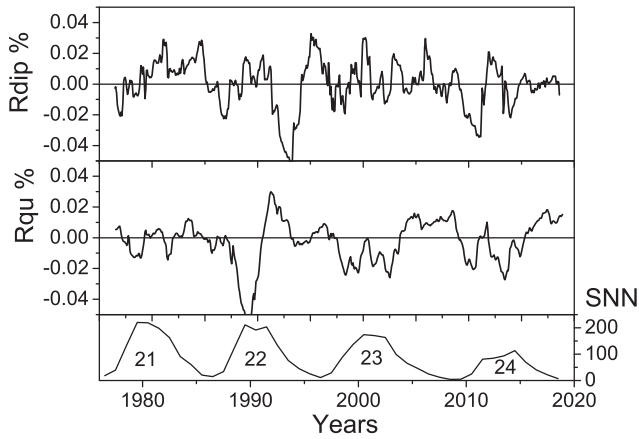


Figure 14. Variations in the dipole and quadrupole rotation rates.

The values obtained, smoothed over 14 rotations, are shown in Fig. 14.

Fig. 14 shows that variations in the rotation rate of a quadrupole range from 0.02–0.06 per cent and display a relationship with the activity cycle. Parameter R is usually negative at the beginning and at the maximum of the cycle and becomes positive in the declining phase and at the minimum. In the case of a dipole, variations in the same range do not show a clear connection, with the cycle being rather chaotic.

Thus, in addition to the secular deceleration of the quadrupole by 0.28 per cent per rotation, we can also observe cyclic variations of five to ten times smaller scale. In the case of the dipole (see above), there are long periods when the rotation rate exceeds the Carrington velocity by about 0.6 per cent and chaotic variations an order of magnitude weaker are observed.

Comparing our findings with available stellar data, we note that Cole et al. (2014) found secular azimuthal dynamo waves in the dipolar field component in their numerical simulations, which show some resemblance to the secular trend seen in solar quadrupolar longitudes. The retrograde migration trend of the solar quadrupole is also reminiscent of similar migration trends found by Lehtinen et al. (2016) for stellar active longitudes, although they reported generally prograde migration. Of course, a self-consistent comparison of stellar and solar data has to be addressed in a particular article.

7 DISCUSSION AND CONCLUSIONS

In this work, we have considered variations of the main components of the large-scale magnetic field: dipole (axial and equatorial, separately) and quadrupole. It is shown that the three main components of the large-scale field behave differently and are not manifestations of the same process.

The axial dipole cannot be fully identified with the polar field; its moment is much lower than the value characteristic of the polar field. The magnitude of the polar field depends not only on the axial dipole but also on higher-order odd harmonics. At polarity reversal, the axial dipole naturally vanishes. However, the period of polarity reversal does not coincide with that of the cycle maximum, as is commonly believed, but occurs 0.5–1 years earlier and takes a very short time.

The characteristics of the equatorial dipole depend to a certain extent (but not entirely) on the contribution of magnetic fields of solar active regions. This contribution is naturally reduced, since, according to the Hale laws, the fields of active regions are associated

with the toroidal field, which is even with respect to the equator. The maximum of the equatorial dipole is shifted from the maximum of the cycle towards the beginning of the declining phase and is quite clearly pronounced. Both axial and the equatorial dipoles have exhibited a systematic decrease during the past four cycles, in agreement with the general decrease of solar activity.

The transition of the pole of a dipole from the polar region to the midlatitudes occurs rather quickly, so that the longitude of the pole changes little. With time, however, this inclined dipole region shifts to higher longitudes, which suggests a weak acceleration of the dipole rotation. The mean rotation rate exceeds the Carrington velocity by 0.6 per cent. Perhaps this is due to the fact that dipole rotation in longitude is determined strictly by the equatorial dipole. According to the differential rotation law, the Carrington velocity corresponds to a latitude of $\pm 26^\circ$, while closer to the equator the rotation rate increases. At shorter time intervals, the dipole displays a random wandering not related in any way to the phase of the cycle.

The behaviour of the quadrupole differs dramatically. Although the quadrupole moment has also decreased for the past four cycles, this decrease was much smaller than that of the dipole moment. As a result, the ratio of the quadrupole and dipole moments has increased for four cycles more than twice, in contrast to sunspot numbers, which displayed a twofold decrease for the same time interval. This reminds us of the situation before the Maunder grand minimum, which, to judge from some indices, had been preceded by an enhancement of the even component of the magnetic field.

It should be noted that using values smoothed over seven rotations (approximately half a year), as in Fig. 8, instead of the mean semiannual values, as in Fig. 6, makes the picture even more interesting. The maxima of the cycles appear as a series of peaks separated by profound dips. The height of the peaks does not decrease at all with time.

The rotation pattern of the quadrupole is more complex and, at the same time, more orderly.

In general, the mean longitude of poles of the same sign decreased by 600° over four cycles, which implies that the mean rotation rate was lower than the Carrington velocity by 0.28 per cent. Secular deceleration is imposed by cyclic variations, with the rotation rate being somewhat lower in the rise phase (by ≈ 0.06 per cent) and becoming positive in the decline phase. These cyclic variations may also be due to the fact that, before the maximum, the pole of the quadrupole is located in the midlatitudes, where the rotation rate is lower than the Carrington velocity, and after the maximum it is located mainly near the equator, where the rotation rate is higher than the Carrington velocity. The secular deceleration may be the result of a gradual shift of the high-latitude boundary between the old and new fields towards lower latitudes, where the rotation rate is lower. For the past four cycles, this boundary has moved from 30° to 20° .³ Now let us see what our analysis says about the symmetry of the magnetic fields generated by the solar dynamo.

On the whole, the solar quadrupole behaves quite differently from the solar dipole and contributes substantially to the total solar magnetic field; however, we do not see specific periods associated with the solar quadrupole, at least during the time under discussion. Correspondingly, it looks plausible that a mode of quadrupole symmetry was not excited on the Sun along with the dipole mode, at least during the time under discussion. Perhaps the most convincing evidence is that the value of the quadrupole moment

³<https://solarscience.msfc.nasa.gov/images/magbfly.jpg>

varies with the same 11-year period as the dipole moment. It seems reasonable to suggest that other differences in the behaviour of dipole and quadrupole moments are due to the fact that deviations of solar hydrodynamics from strict symmetry about the equator have different effects on the dipole and quadrupole components. In any case, we do not see here dramatic phenomena such as the occurrence of sunspots almost exclusively in one solar hemisphere, as was observed at the end of the Maunder minimum.

Finding out how minor deviations from symmetry about the equator lead to differences in the behaviour of the dipole and quadrupole fields and how frequent these deviations are in the Sun would require special analysis of observations and numerical modelling, which is far beyond the scope of this article.

At the same time, we cannot ignore the fact that the current behaviour of the solar magnetic field differs noticeably from what was observed over the past century (e.g. de Jager et al. 2016), so it is possible that the Sun is approaching a new Grand Minimum. We have no opportunity to check whether the particularities of the quadrupole behaviour described above were typical throughout the past century. On the other hand, we do not know what exactly happened to the Sun just before the Maunder minimum, since the observation data available are not very definite (see Usoskin et al. 2015; Zolotova & Ponyavin 2015). However, these data also sometimes display signatures of significant asymmetry in the distribution of sunspots relative to the solar equator (Nesme-Ribes et al. 1994).

Notwithstanding all limitations, we can conclude that at present there is no reason to believe that either quadrupole or mixed parity magnetic configurations are excited in the Sun along with the main dipole mode. The occurrence of quadrupole and other even harmonics is more rightfully attributed to deviations of solar hydrodynamics from strict symmetry with respect to the solar equator.

ACKNOWLEDGEMENTS

We acknowledge the help of the Wilcox Solar Observatory. Data used in this study were obtained via the website <http://wso.stanford.edu/>, courtesy of J. T. Hoeksema. This work was supported by the RFBR grants 17-02-00300, 19-02-00191a, 19-52-53045 and 18-02-00085.

REFERENCES

Brandenburg A., 2005, *ApJ*, 625, 539
 Brandenburg A., Sokoloff D., Subramanian K., 2012, *Space Sci. Rev.*, 169, 123
 Böhm-Vitense E., 2007, *ApJ*, 657, 486

Choudhuri A. R., 1990, *ApJ*, 355, 733
 Cole E., Käpylä P. J., Mantere M. J., Brandenburg A., 2014, *ApJ*, 780, L22
 de Jager C., Akasofu S.-I., Duhau S., Livingston W. C., Nieuwenhuijzen H., Potgieter M. S., 2016, *Sci. Rev.*, 201, 109
 De Rosa M. L., Brun A. S., Hoeksema J. T., 2012, *ApJ*, 757, 96
 Gigolashvili M. Sh., Khutsishvili E. V., 1990, In ESA, Plasma Astrophysics (SEE N91-15046 06-90), ESA Publications Division, Noordwijk, The Netherlands, p. 35
 Hathaway D. H., Wilson R. M., 1980, *ApJ*, 357, 271
 Hoeksema J. T., 1991, Report CSSA-ASTRO-91-01, Center for Space Science and Astrophysics, Stanford, CA
 Hoeksema J. T., Scherrer P. H., 1986, WDCA Report UAG-94, NGDC, Boulder, CO
 Howard R., 1984, *ARA&A*, 22, 131
 Jennings R. L., Weiss N. O., 1991, *MNRAS*, 252, 249
 Kambry M. A., Nishikawa J., 1990, *Solar Phys.*, 126, 89
 Knaack R., Stenflo J. O., 2005, *A&A*, 438, 349
 Krause F., Rädler K.-H., 1980, Mean-field Magnetohydrodynamics and Dynamo Theory, Pergamon Press, Oxford
 Lehtinen J., Jetsu L., Hackman T., Kajatkari P., Henry G. W., 2016, *A&A*, 588, A38
 Livshits I. M., Obridko V. N., 2006, *Astron. Rep.*, 50, 926
 Moss D., Kitchatinov L. L., Sokoloff D., 2013, *A&A*, 550, L9
 Moss D., Saar S. H., Sokoloff D., 2008, *MNRAS*, 388, 416
 Nesme-Ribes E., Sokoloff D., Ribes J. C., Kremlivsky M., 1994, in Nesme-Ribes E., ed., The Solar Engine and its Influence on Terrestrial Atmosphere and Climate. Springer-Verlag, Berlin Heidelberg, p. 71
 Noyes R. W., Weiss N. O., Vaughan A. H., 1984, *ApJ*, 287, 769
 Obridko V. N., Shelting B. D., 2016, *Astron. Lett.*, 42, 631
 Obridko V. N., Shelting B. D., Kharshiladze A. F., 2006, *Geomagn. Aeron.*, 46, 294
 Pipin V. V., Moss D., Sokoloff D., Hoeksema J. T., 2014, *A&A*, 567, A90
 Pizzolato N. et al., 2003, *A&A*, 397, 147
 Reiners A., Basri G., Browning M., 2009, *ApJ*, 692, 538
 Ribes J.-C., Nesme-Ribes E., 1993, *A&A*, 276, 549
 Rosén L., Kochukhov O., Hackman T., Lehtinen J., 2016, *A&A*, 593, A35
 Rosén L., Kochukhov O., Alecian E., Neiner C., Morin J., Wade G. A., BinaMcS Collaboration, 2018, *A&A*, 613, A60
 Saar S. H., Brandenburg A., 1999, *ApJ*, 524, 295
 Scherrer P. H., Wilcox J. M., Svalgaard L., Duvall T. L. Jr., Dittmer P.H., Gustafson E. K., 1977, *Solar Phys.*, 54, 353
 See V., et al., 2016, *MNRAS*, 462, 4442
 Sokoloff D., Nesme-Ribes E., 1994, *A&A*, 288, 293
 Stenflo J. O., Güdel M., 1988, *A&A*, 191, 137
 Stenflo J. O., Vogel M., 1986, *Nature*, 319, 285
 Stenflo J. O., Weisenhorn A. L., 1987, *Solar Phys.*, 108, 205
 Usoskin I. G., et al., 2015, *A&A*, 581, A95
 Wang Y. M., Sheeley N. R., 1992, *ApJ*, 392, 310
 Zolotova N. V., Ponyavin D. I., 2015, *ApJ*, 800, 42

This paper has been typeset from a $\text{\TeX}/\text{\LaTeX}$ file prepared by the author.